engineering proceedings

MDPI

Proceeding Paper

Structural, Morphological and Mechanical Properties of Concrete Slab in Traditional Buildings, Case Study: Casablanca-Morocco †

H. Soumadrass *, Z. Beidouri and Kh. Zarbane

LARILE, Higher Institute of Technology, Hassan II University, Casablanca, Morocco;
zbeidouri@gmail.com (Z.B.); khalidzarbane@gmail.com (K.Z.)
* Correspondence: hsoumadrass@gmail.com

† Presented at the 4th International Electronic Conference on Applied Sciences, 27 October–10 November 2023; Available online: https://asec2023.sciforum.net/.

Abstract: Morphological, structural and mechanical analyses were performed on reinforced concrete slab samples used in traditional buildings in Casablanca, Morocco. X-ray diffraction and morphological analysis revealed that all samples had a low Ca/Si intensity, which could be the primary factor responsible for the reduction in compressive strength of our samples. The compressive strength ranges between 30.5 and 29.1 MPa, and the flexural strength ranges between 13 and 15 MPa. These results aim to obtain the basic knowledge necessary to propose a correct diagnosis, useful for planning conservation projects compatible with the specificity of the local culture of the building.

Keywords: traditional buildings; concrete slab; elasticity modulus; mechanical properties: sclerometer test; porosity; Ca/Si ratio

Citation: Soumadrass, H.; Beidouri, Z.; Zarbane, K. Structural, Morphological and Mechanical Properties of Concrete Slab in Traditional Buildings, Case Study: Casablanca-Morocco. *Eng. Proc.* **2023**, *52*, x. https://doi.org/10.3390/xxxxx

Academic Editor(s): Name

Published: date

1. Introduction

The improvement of concrete slabs is a typical requirement for the restoration of old buildings [1,2]. Over time, these buildings present a variety of pathologies, due to lack of maintenance, climatic conditions, as well as construction technology [3]. It is well known that the life span of a concrete structure depends on many factors of physical, chemical or biological origin that can accelerate its deterioration [4]. Before any intervention, it is essential to perform a preliminary analysis and laboratory tests to evaluate the performance of old structures. According to the literature, Chen et al. [5] studied how temperature affects the dynamic mechanical properties of concrete. The results showed that the dynamic strength increased as the strain rate increased. Cruz et al. [6] investigated the chemical and physical characterization of ancient concrete built in 1907, the average modulus of elasticity was found to be 30 GPa and the strength class was revealed to be higher than C30/37. Qazweeni et al. [7] studied the physical, chemical, and mechanical properties of old concrete structure. The used concrete had high voids and absorption ratios, as well as a low density and a wide scatter in compressive strength results. Prassianakis et al. [8] used destructive and ultrasonic nondestructive testing methods to determine the mechanical properties of old concrete. Ambroziak et al. [9] revealed the durability and strength of concrete continuous footings based on the concrete's physical, chemical, and mechanical properties. Large dispersions of the cylindrical compressive strength (6.9–29.3 MPa), density (1750–2100 kg = m^3), and water absorption (5–14%) were observed. Gibas et al. [10] investigated the compressive strength of cored concrete specimens. The compressive strength was greater than 60 MPa. As a result, the subject of old concrete structures is being studied in a variety of technical and scientific studies, using a variety of methods and laboratory tests to determine their properties. The lack of universal tools for describing the behavior of old concrete suggests the need for new research and laboratory experiments. A correct assessment of the properties of old concrete is required to ensure the life span of old structures. In this context, Morphological, structural, and mechanical analyses were performed on reinforced concrete slab samples used in traditional buildings.

2. Experimental

2.1. X-ray Diffraction Analysis (XRD)

The samples were characterized by X-ray diffraction analysis (XRD) with model (A Siemens D-501 X-ray diffraction (XRD) instrument, $CuK_{\alpha1}$, λ = 1.540598 Å) at room temperature. Data was collected in the 2θ range of 20° to 80° with a step size of 0.0167° and a count time of 18 s/step.

2.2. Scanning Electron Microscopy (SEM) and Energy Dispersive X-rays (EDX)

The chemical morphology of all samples was analyzed using scanning electron microscopy (SEM) and energy dispersive X-ray (EDX) techniques (The FEI Quanta450 FEG environmental scanning electron microscope (ESEM)).

2.3. Hydrostatic Balance Test

According to NF EN 1097-6: 2001, we placed all of the samples in the hydrostatic balance's suspension system, in which they were completely immersed and weighed at 0.01% in water and air to calculate the mass (M_{water}) and mass in air (M_{air}). Furthermore, all samples were dried at (1055) °C until they reached a constant mass (the dry mass (M_{dry})). The following formula was used to calculate bulk density (kg/m^3) and water accessible porosity (%): (ρ_w: density of water (kg/m^3).

$$\rho = \frac{M_{\text{dry}}}{M_{\text{air}} - M_{\text{water}}} \quad (1)$$

$$\text{n} = \frac{M_{\text{air}} - M_{\text{dry}}}{M_{\text{air}} - M_{\text{water}}} \times 100 \quad (2)$$

2.4. Sclerometer Test

To perform this test, we took into account the Moroccan standard NM 10-1-008 [11], which defines an appropriate performance. In order to start the test, the evaluated areas were dried and polished with a prism to obtain a smooth finish on the surface. An Original Schmidt PROCEQ type PT hammer was used. A total of five tests per post were recorded (Figure 2).

2.5. Identification of Compressive and Flexural Strength

The specimens' compressive strength was determined after compression and bending tests in accordance with European standard EN 196-1. Six fragments were obtained from four specimens of varying sizes (2 for each specimen). Each fragment's compressive strength was tested, and the average result of the two fragments was calculated.

2.6. Identification of Elasticity Modulus

According to the European standard "EN 12390-13: 2013", the specimen is placed with the measuring equipment fixed axially in the middle of the testing machine. The preload stress (stress) p is applied. This stress is maintained for a maximum of 20 **s**. At the end of this period, the strain measuring equipment is reinstalled. The strain of each measuring line is recorded and the average strain ε is calculated using the formula below [12]:

$$\varepsilon = \frac{\Delta l}{l_0} \quad (3)$$

where $\boldsymbol{l_0}$ is the initial length, $\boldsymbol{l_f}$ is the final length and the $\Delta \boldsymbol{l}$ the variation in concrete slab length.

3. Results and Discussions

3.1. X-Ray Diffraction Analysis

XRD measurements of our samples are shown in Figure 1. The observed diffraction peaks show a low intensity of Ca/Si for all the samples studied. It can be noted that the Ca/Si ratio is one of the factors contributing to the compressive strength. According to Tob'on et al. [13], the amount of Ca/Si is the main parameter at later hydration ages. The spacing values obtained at the Ca/Si vertex is highly correlated with the results obtained [14]. According to the XRD analyses, the trend of the maximum Ca/Si values is in good agreement with the compressive strengths and the Ca/S ratio.

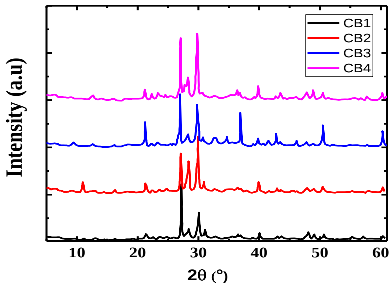

Figure 1. XRD pattern for different specimens of Concrete slab.

3.2. Scanning Electron Microscopy (SEM)

SEM-EDX analysis was performed on the different concrete slabs shown in Figure 2. SEM-EDX analysis revealed that the samples contain C-S-H gel, small amounts of carbon and sulfur, Ca/Si ratio and different morphologies. The presence of sulfur in the specimens shows that the concrete is corroding at the reinforcement level. It can be noted that the increase in compressive strength is related to the increase in Ca/Si ratios. This result is consistent with that found by X-ray diffraction results. In addition, other factors may influence the low compressive strength value of the samples, such as porosity, poor aggregate-paste adhesion aggravated by bleeding, and water lenses under the aggregate particles [15].

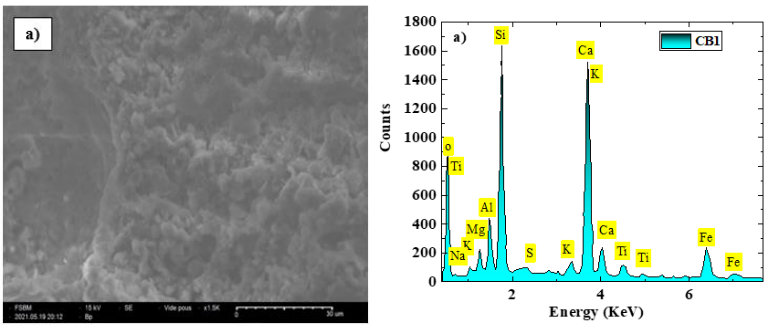

Figure 2. SEM and EDX of concrete slab specimen (CB1).

3.3. Apparent Density and Porosity Accessible to Water

The bulk density of the concrete slab depends on several essential parameters such as: the weight of the cement and the planer, the density of the quarry sand, the amount of air and water trapped. We calculated the bulk density using Equation (1). We found the value to be between 1642.8 kg/m³ and 1503.4 kg/m³, respectively (Table 1). This can be explained by the rate of water absorption [16]. The structure that contains these samples makes the building very damaged and in danger of collapsing. This result is due to the decrease in the compactness of the concrete slabs. The increase in the porosity of the mortars in the hardened state leads to a decrease in their density (Figure 3a). Poor dispersion in the matrix is also observed when agglomerated particles are found to cause the formation of a "ball" presented at certain points in the composite [17]. The high water absorption (Figure 3b) rate of concrete slabs and their microporous structure increase the porosity of the composite [18].

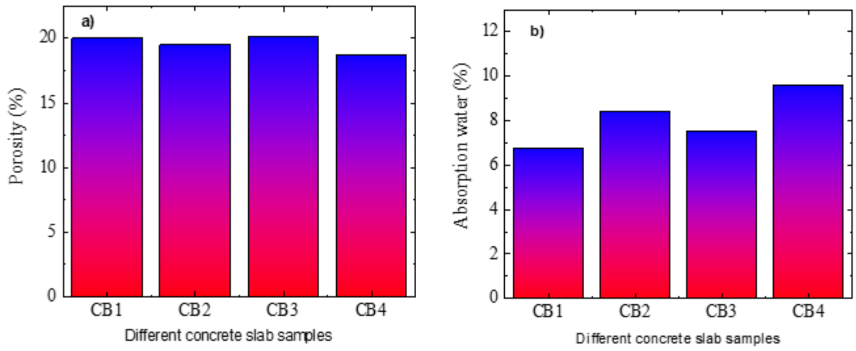

Figure 3. (**a**) Porosity and (**b**) Absorption water for different Concrete slab samples.

Table 1. Hydrostatic balance test of concrete slab samples used in traditional buildings in Casablanca, Morocco.

Samples	Dry Mass M_d (g)	Density × 10⁶ (g/cm³)	Absorption by Mass (%)
CB1	7 468.5	1.6428	6.76
CB2	8 412.5	1.5809	8.43
CB3	8 344.3	1.5034	7.55
CB4	7 645.5	1.5383	9.63

3.4. Sclerometer Test

Table 2 displays the experimental values for the sclerometric compressive strength. It should be noted that the sclerometric compressive strength for the beams is an average of 5.8 MPa, while the column is an average of 18.9 MPa. Furthermore, the mean value derived from the sclerometric compressive strength of the concrete slab is 30.2 MPa, which is low when compared to the recommended values for this type of structure [15,20]. This low sclerometric compressive strength value is due to the material structure of these traditional buildings, which is composed of weak concrete translated by the low dosage of cement mode 35, so that insufficient length of the anchor can influence the reduction of compressive strength and thus poses the failure problem [13].

Table 2. Results obtained by sclerometer test for concrete slab samples.

Samples	Young Module (Mpa)	Compression Strength (MPa)	Flexion Strength (MPa)
CB1	15.2	27.6	4.5
CB2	6.4	16.3	3.2
CB3	13.1	17.2	3.5
CB4	5.7	12.3	2.7

3.5. Compressive Strength

Figure 4 depicts the compressive strength test results for the various concrete slabs. According to Table 3, the average value for compressive strength is between 30.5 and 29.1 MPa. This result is comparable to that obtained by measuring the resistance to scelometric compression and lower to that obtained with existing concrete slabs [21]. On the other hand, the difference in values found for each sample is compatible with the Ca/Si ratio determined by EDX and XRD analysis.

3.6. Elasticity Modulus

The extracted Young's modulus measurements for the different samples are presented in Table 3. The values obtained vary between 5 and 7.6 MPa and are very low compared to the value obtained in the previous study [22]. This is due to the difference in porosity and density for each concrete slab studied. Other factors influencing Young's modulus are hardening, age, aggregate type and water-cement ratio, and Ca/Si ratio.

3.7. Flexural Tensile Strength

The flexural strength tests of the concrete slab are shown in Figure 4. The obtained values are presented in Table 3. As can be seen; the obtained flexural strength values vary between 13 and 15 MPa, respectively. This result is lower than that of the existing concrete slab [23]. The results is interpreted that many carboxylic acids are known to be strong retarders based on the EDX measurement.

Table 3. Mechanical properties of concrete slab samples used in traditional buildings in Casablanca, Morocco.

Samples	Standard Deviation (Mpa)	Compression Resistance Sclerometer (MPa)
column 1	1.4	6.3
column 2	1.4	5.3
Beam 1	2.8	15.9
Beam 2	1.6	21.3
CB1	1.2	27.5
CB2	1.2	16.5
CB3	1.3	26.3
CB4	1.4	12.4

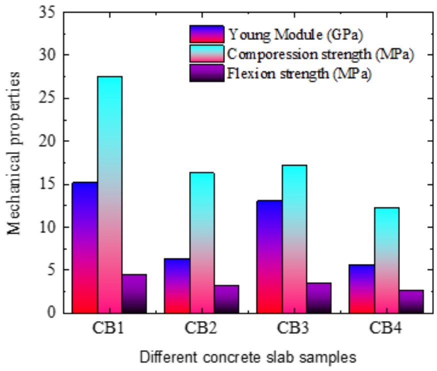

Figure 4. Mechanical properties for Different Concrete slab samples.

4. Conclusions

The article presents the results of a study on the concrete slab of the Medina of Casablanca, an important city in the cultural heritage of Morocco. These results aim to obtain the basic knowledge necessary to propose a correct diagnosis, useful for planning conservation projects compatible with the specificity of the local culture of the building. In particular, this work focuses on the study of morphological, structural and mechanical characteristics of the concrete slab. Different parameters are obtained such as apparent density, porosity, compressive strength, elasticity modulus and flexural strength.

Author Contributions: All authors have read and agreed to the published version of the manuscript.

Funding: This research received no external funding.

Institutional Review Board Statement: Not applicable.

Informed Consent Statement:

Data Availability Statement: No new data were created.

Conflicts of Interest: The authors declare no conflict of interest.

References

1. Devi, C.; Vijayan, D.S.; Nagalingam, R.; Arvindan, S. A review of the implementations of glass fiber in concrete technology. *Mater. Today Proc.* **2022**, *62*, 2010–2015. https://doi.org/https://doi.org/10.1016/j.matpr.2022.02.293.
2. Karumanchi, M.; Bellum, R.R.; Chennupati, M.; Kunchala, V.; Regulagunta, M. Influence on mechanical properties of concrete of cement replacement with fly ash and river sand replacement with foundry sand. *Mater. Today Proc.* **2022**, *65*, 3547–3551. https://doi.org/https://doi.org/10.1016/j.matpr.2022.06.146.
3. Resende, M.M.; Gambare, E.B.; Silva, L.A.; de S, Y.; Almeida, E.; Salvador, R.P. Infrared thermal imaging to inspect pathologies on façades of historical buildings: A case study on the Municipal Market of São Paulo, Brazil. *Case Stud. Constr. Mater.* **2022**, *16*, e01122. https://doi.org/https://doi.org/10.1016/j.cscm.2022.e01122.
4. Jia, H.; Qiao, G.; Han, P., Machine learning algorithms in the environmental corrosion evaluation of reinforced concrete structures—A review. *Cem. Concr. Compos.* **2022**, *133*, 104725. https://doi.org/https://doi.org/10.1016/j.cemconcomp.2022.104725.
5. Chen, C.; Xudong, C.; Xiaojing, L. Dynamic Compressive Behavior of 10-Year-Old Concrete Cores after Exposure to High Temperatures. *J. Mater. Civ. Eng.* **2020**, *32*, 4020076. https://doi.org/10.1061/(ASCE)MT.1943-5533.0003156.
6. Sena-Cruz, J.; Ferreira, R.M.; Ramos, L.F.; Fernandes, F.; Miranda, T.; Castro, F. Luiz Bandeira Bridge: Assessment of a Historical Reinforced Concrete (RC) Bridge. *Int. J. Archit. Herit.* **2013**, *7*, 628–652. https://doi.org/10.1080/15583058.2012.654895.
7. Qazweeni, J.A.; Daoud, O.K. Concrete deterioration in a 20-year-old structure in Kuwait. *Cem. Concr. Res.* **1991**, *21*, 1155–1164. https://doi.org/https://doi.org/10.1016/0008-8846(91)90076-T.
8. Prassianakis, I.N.; Giokas, P. Mechanical properties of old concrete using destructive and ultrasonic non-destructive testing methods. *Mag. Concr. Res.* **2003**, *55*, 171–176. https://doi.org/10.1680/macr.2003.55.2.171.
9. Andrzej, A.; Elzbieta, H.; Jaroslaw, K. Chemical and Mechanical Properties of 70-Year-Old Concrete. *J. Mater. Civ. Eng.* **2019**, *31*, 4019159. https://doi.org/10.1061/(ASCE)MT.1943-5533.0002840.
10. Gibas, K.; Glinicki, M.A.; Jóźwiak-Niedźwiedzka, D.; Dąbrowski, M.; Nowowiejski, G.; Gryziński, M. Properties of the Thirty Years Old Concrete in Unfinished Żarnowiec Nuclear Power Plant. *Procedia Eng.* **2015**, *108*, 124–130. https://doi.org/https://doi.org/10.1016/j.proeng.2015.06.127.
11. Šimonová, H.; Daněk, P.; Frantík, P.; Keršner, Z.; Veselý, V. Tentative Characterization of Old Structural Concrete through Mechanical Fracture Parameters. *Procedia Eng.* **2017**, *190*, 414–418. https://doi.org/https://doi.org/10.1016/j.proeng.2017.05.357.
12. Noufid, A.; Hidar, N.; Belattar, S.; Elafi, M.; Feddaoui, M. Valorization of polypropylene fibers to improve the physical and mechanical properties of concrete and mortars. *Res. Sq.* **2022**, 1–23. https://doi.org/10.21203/rs.3.rs-2002272/v1.
13. Bheel, N.; Mahro, S.K.; Adesina, A. Influence of coconut shell ash on workability, mechanical properties, and embodied carbon of concrete. *Environ. Sci. Pollut. Res.* **2021**, *28*, 5682–5692. https://doi.org/10.1007/s11356-020-10882-1.
14. Rehman, S.K.U.; Ibrahim, Z.; Memon, S.A.; Jameel, M. Nondestructive test methods for concrete bridges: A review. *Constr. Build. Mater.* **2016**, *107*, 58–86. https://doi.org/10.1016/j.conbuildmat.2015.12.011.
15. Escalante-García, G.M.-S.J.I.; Fuentes, A.F.; Gorokhovsky, A.; Fraire-Luna, P.E. Hydration Products and Reactivity of Blast Furnace Slag Activated by Various Alkalis. *J. Am. Ceram. Soc.* **2003**, *86*, 2148–2153. https://doi.org/10.1111/j.1151-2916.2003.tb03623.x.
16. Bekdaş; G; Sayin, B.; Çelik Sola, Ö.; Güner, A. Assessment of the material quality of damaged structures after earthquake in Van, Turkey. *J. Mater. Civ. Eng.* **2016**, *28*, 04016110.
17. Lo, F.-C.; Lo, S.-L.; Lee, M.-G. Effect of partially replacing ordinary Portland cement with municipal solid waste incinerator ashes and rice husk ashes on pervious concrete quality. *Environ. Sci. Pollut. Res.* **2020**, *27*, 23742–23760. https://doi.org/10.1007/s11356-020-08796-z.
18. Kaplan, G.; Gulcan, A.; Cagdas, B.; Bayraktar, O.Y. The impact of recycled coarse aggregates obtained from waste concretes on lightweight pervious concrete properties. *Environ. Sci. Pollut. Res.* **2021**, *28*, 17369–17394. https://doi.org/10.1007/s11356-020-11881-y.

19. Zhuang, S.; Wang, Q.; Zhang, M. Water absorption behaviour of concrete: Novel experimental findings and model characterization. *J. Build. Eng.* **2022**, *53*, 104602. https://doi.org/10.1016/j.jobe.2022.104602.
20. Kancharla, R.; Maddumala, V.R.; Prasanna, T.V.N.; Pullagura, L.; Mukiri, R.R.; Prakash, M.V. Flexural Behavior Performance of Reinforced Concrete Slabs Mixed with Nano- and Microsilica. *J. Nanomater.* **2021**, *2021*, 1754325. https://doi.org/10.1155/2021/1754325.
21. Alemu, A.S.; Yoon, J.; Tafesse, M.; Seo, Y.-S.; Kim, H.-K.; Pyo, S., Practical considerations of porosity, strength, and acoustic absorption of structural pervious concrete. *Case Stud. Constr. Mater.* **2021**, *15*, e00764. https://doi.org/10.1016/j.cscm.2021.e00764.
22. Choi, S.-H.; Hwang, J.-H.; Han, S.-J.; Cho, H.-C.; Kim, J.H.; Kim, K.S. Simplified Effective Compressive Strengths of Columns with Intervening Floor Slabs. *Int. J. Concr. Struct. Mater.* **2020**, *14*, 42. https://doi.org/10.1186/s40069-020-00419-8.
23. Hanchak, S.J.; Forrestal, M.J.; Young, E.R.; Ehrgott, J.Q. Perforation of concrete slabs with 48 MPa (7 ksi) and 140 MPa (20 ksi) unconfined compressive strengths. *Int. J. Impact Eng.* **1992**, *12*, 1–7. https://doi.org/10.1016/0734-743X(92)90282-X.